



NUMERICAL MODELING OF GAS LEAKAGE THROUGH DAMAGED COMPOSITE LAMINATES

Hisashi Kumazawa*, John Whitcomb** [Hisashi Kumazawa]:kumazawa.hisashi@jaxa.jp
*Structure Technology Center, Japan Aerospace Exploration Agency
**Department of Aerospace Engineering, Texas A&M University

Keywords: *laminates, leakage, finite element analysis, cracks, delamination, cryogenic tank*

Abstract

A numerical model of leakage through a damaged laminate was developed. The model utilized crack openings determined by the finite element method (FEM). The gas flow was simulated using computational fluid dynamics (CFD). Delamination length at crack intersections was estimated based on experimental data for specimens subjected to thermal loads only. Leakage under biaxial mechanical loadings was predicted with the estimated delamination length. CFD models, in which crack opening displacements (COD) were assumed to follow a polynomial shape, overestimated the permeability of biaxial specimens. Flat crack CFD models, in which CODs are assumed to be constant through the ply thickness as an approximation of the higher resistance in rough surface cracks, underestimated the permeability.

1 Introduction

Vehicle weight reduction is critical in the development of low-cost transportation systems to space, such as the reusable rockets and the latest generation of expendable launch vehicles. Reduction of the cryogenic propellant tank weight is particularly important, since a large part of the vehicle is occupied by the tanks. Many research and development efforts have focused on the application of composite materials to the cryogenic tanks for the purpose of achieving significant vehicle weight reduction, such as the X-33 advanced technology demonstrator [1]. During preflight proof testing, the X-33 liquid hydrogen tank failed due to disbonds and separation of the facesheets from the core material when the pressure increased in the core of the sandwich tank wall. Investigation of causes of the failure was performed and an investigation team determined the most probable cause of the failure to

be a combination of reduced bondline strength between facesheets and honeycomb core and microcracking of the inner facesheet with subsequent accumulation of gases in the honeycomb core [2].

After the failure of the X-33 liquid hydrogen tanks, trade studies on structural design of composite material tanks for reusable rockets were conducted to determine permeability requirements and to develop improvements of materials, design, and manufacturing [3, 4]. These trade studies concluded that matrix cracking at cryogenic temperature and fuel leakage through the matrix cracks are very important considerations in the design of composite tanks for the reusable rockets. Thus it is worthwhile to evaluate formation of the matrix cracks under cryogenic temperature and gas leakage through the damaged composite materials for the cryogenic propellant tanks. Based on coupon level experimental tests at cryogenic temperatures, it was concluded that matrix cracks occur at relatively low mechanical loads under cryogenic environment and these cracks might cause propellant leakage [5, 6].

The relationship between damage and leakage has been investigated for the cryogenic propellant tanks. The effects of the cryogenic temperature and the mechanical load on leakage through the composite laminates have been experimentally evaluated by several research groups. Kumazawa *et al.* measured leakage through composite laminates under biaxial loadings using cruciform specimens at room temperature [7-10]. Results of the experiments indicated close relationships between an increase of permeability and applied tensile loads. Humpenoder [11] and Vernon *et al.* [12] measured permeability through composite laminates at room and cryogenic temperature. The results showed that permeability at room temperature was much lower than at cryogenic temperature because the damage state was much different. At room temperature there was much less

damage and no continuous leakage path through thickness, so the “leakage” was by diffusion only. The much more extensive damage at cryogenic temperature resulted in a continuous leakage path.

Kumazawa *et al.* [9, 10] developed a leak analysis based on crack opening displacements in cross-ply laminates. Comparison between numerical calculations and experimental leakage data under biaxial loadings indicated that the predictions are in good agreement with the experimental data. Enlargement of the crack opening by changing the loads was shown to increase permeability. In the leak analysis, an empirical constant was used to quantify the relationship between crack opening displacements and leak resistance at the intersections of transverse matrix cracks. The value of the constant was chosen to account for damages, such as delamination, near the crack intersection. Yokozeki

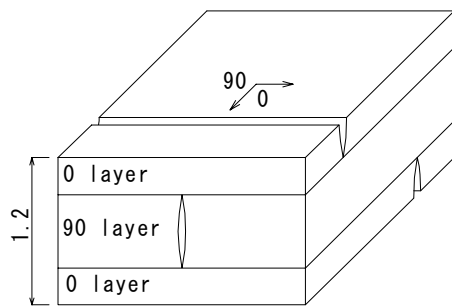


Fig. 1. Matrix cracks in a damaged laminate

Table 1. Elastic constants of IM600/#133 CF/epoxy

Property	
E_L (GPa)	147.1
E_T (GPa)	8.12
G_{LT} (GPa)	4.50
G_{TT} (GPa)	3.00
ν_{LT}	0.35

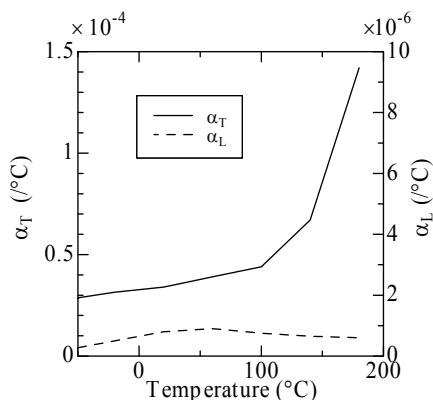


Fig. 2 Thermal expansion coefficients of IM600/#133 CF/Epoxy

et al. [13] investigated the effect of intersection angle of matrix cracks on leakage, and reported the constant is a function of intersection angle. Roy *et al.* [14, 15] developed a leakage analysis that considered delaminations at crack intersections, and calculated the effects of temperature change, mechanical loadings and delamination length at the crack intersection on permeability.

In this study, a numerical model of leakage through the damaged laminate is developed. The leakage simulation is composed of calculations of crack opening displacements in the damaged laminate and of gas flow through the damage network acting as a leak path. Numerical results are compared with experimental data to evaluate the effectiveness of the numerical model.

2 Leakage through Damaged Laminates

Peddiraju *et al.* [16] calculated hydrogen leakage through a damaged composite laminate. Matrix crack opening displacements in the damaged laminate, which provide part of the leakage path, were calculated by using three dimensional finite element analysis (FEA). The leakage was calculated by using the commercial computational fluid dynamics (CFD) software Fluent (Fluent, Inc.) with the assumption that hydrogen behaved as an incompressible fluid. The comparison of predictions and experimental data indicated that the numerical method had the potential to predict the leakage through damaged laminates. However, validation of the numerical modeling of gas leakage was not possible because of uncertainties about crack densities in the experimental data.

In the current study, the gas is assumed to be compressible for improvement of the numerical modeling. For further validation of the modeling, numerical results are compared with experimental data from [9], which reported the crack density and leakage at room temperature.

3 Finite Element Analysis

The leakage through a damaged $(0_2/90_2)_S$ laminate is calculated. The thickness of the laminate was 1.2mm. The material was carbon fiber/180°C cured epoxy IM600/#133. Helium gas flow through the damage network, which consisted of matrix cracks in all layers (see Fig. 1) and delaminations at the intersections of the matrix cracks, was calculated

by using Fluent. The FEA was used to determine the dimensions of the leakage path.

3.1 Material Properties

The orthotropic elastic constants and coefficients of thermal expansion (CTE) of IM600/#133 are shown in Table 1 and Fig. 2[9], respectively. The symbols E , G , ν , α_L , and α_T are

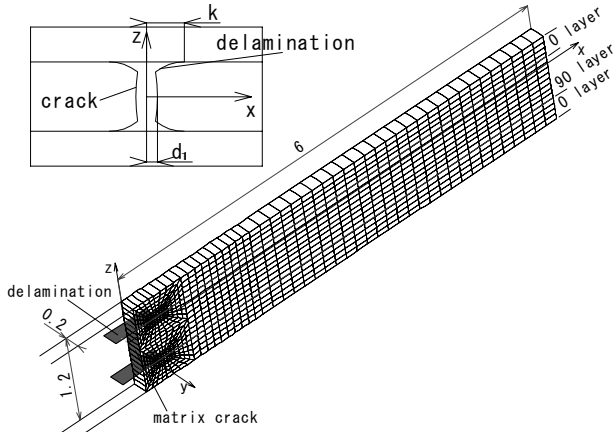


Fig. 3. Finite element mesh of half model (crack in 90 layer, delamination length = 0.3mm)

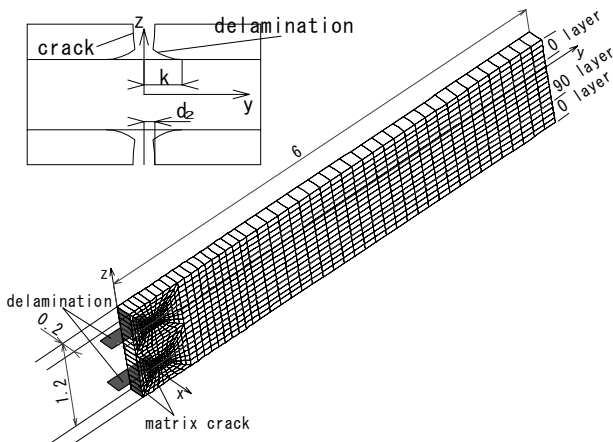


Fig. 4. Finite element mesh of half model (crack in 0 layer, delamination length = 0.3mm)

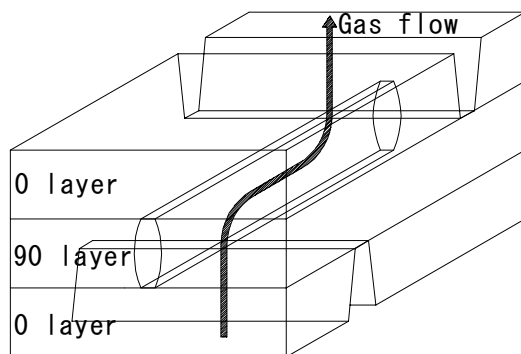


Fig. 5. Gas flow through matrix cracks

refer to extensional modulus, shear modulus, Poisson's ratio, longitudinal CTE and transverse CTE, respectively. The stress free temperature T_0 is assumed to be 100°C, which was estimated stress free temperature from measured leakage in [10].

3.2 Finite Element Models

The crack opening displacements due to thermal and biaxial mechanical loading were calculated by three dimensional FEA. Numerical results in [16] revealed that the effect of cracks in adjacent layers on the crack opening displacements is small in cross-ply laminates. In this study, the crack opening displacements in each layer are approximately calculated using a finite element mesh with no crack in the adjacent layers (Figs. 3 and 4). The dimensions of the delamination adjacent to the matrix crack and crack opening displacements in 90° and 0° layers are defined as k , d_1 and d_2 as shown in Figs. 3 and 4. In this paper, x and y axes coincide with the 0° and 90° directions of laminates respectively, and the z axis is the direction through the ply thickness.

A typical finite element model used for this study consists of 20-node brick elements. Both thermal and biaxial mechanical loads were considered. Periodic boundary conditions were imposed on unit cells. For the configuration with cracks in the 90° layer, the surfaces parallel to the x - z plane and the surface parallel to the y - z plane except for the cracked region are flat due to symmetry (Fig. 3). The boundary conditions are expressed as follows:

$$u(x=0, y, z | z < -0.3, 0.3 < z) = 0 \quad (1)$$

$$u(x=6, y, z) = 6 \langle \epsilon_x \rangle \quad (2)$$

$$v(x, y=0, z) = 0 \quad (3)$$

$$v(x, y=0.2, z) = 0.2 \langle \epsilon_y \rangle \quad (4)$$

where u , v , w , and $\langle \epsilon_i \rangle$ ($i=x, y$) are x -, y - and z -directional displacements and i -directional volume averaged normal strains, respectively[17].

Similarly, boundary conditions for the finite element models with 0 layer cracks (Fig. 4) are expressed as follows:

$$u(x=0, y, z) = 0 \quad (5)$$

$$u(x=0.2, y, z) = 0.2 \langle \epsilon_x \rangle \quad (6)$$

$$v(x, y=0, z | -0.3 < z < 0.3) = 0 \quad (7)$$

$$v(x, y=6, z)=6\langle\varepsilon_y\rangle \quad (8)$$

When determining crack opening displacements under thermal load, the volume average strains $\langle\varepsilon_i\rangle$ ($i=x, y$) are also calculated as part of the solution process. When the loading was biaxial strain, the volume average strains $\langle\varepsilon_i\rangle$ ($i=x, y$) are specified as part of the input data. Crack opening displacements under combined thermal and the mechanical loads are obtained by superposition.

4 Computational Fluid Dynamic Analysis

4.1 Fluent Model

Helium gas flows through the damage network which is composed of matrix cracks in all layers as shown in Fig. 5. Compressible, viscous, laminar gas flow through the damage network was calculated using Fluent, which employs the Finite Volume Method. The crack pattern is assumed to be periodic as shown in Figs. 6 and 7. Experimental and numerical research [18, 19] reported that matrix cracks in the 0° layer in $(0_n/90_m)_s$ laminates commonly locate at staggered positions as shown in Fig. 7. Unit cells for calculation by Fluent are shown in Figs. 6 and 7. The matrix cracks of the surface 0° layers in Fig. 6 are aligned, but in Fig. 7 they are offset. Gas flow is induced by a pressure difference of 1.0×10^5 Pa between the two surfaces of the laminate, which also was the condition for the experiments in [9]. A typical grid for the CFD analysis is shown in Fig. 8. The grid is more refined near crack intersections than in other regions.

4.2 Estimation of Delamination Length

Two intersecting cracks have no overlapping area if there is no delamination, which would result in much less leakage than has been observed in experiments. Hence, a delamination was assumed at all intersections of matrix cracks. However, it is difficult to experimentally measure the delamination length near crack tips. In this study, an appropriate delamination length is estimated by comparison of predicted and experimentally measured leakage under thermal loading.

The appropriate delamination length was obtained by trial and error. First, FEA was used to calculate crack opening displacements for an assumed delamination of dimension 0.3mm. The leakage rate was determined for a CFD model based on the FEA. If the calculated leakage was larger than the experimental results, the next assumed

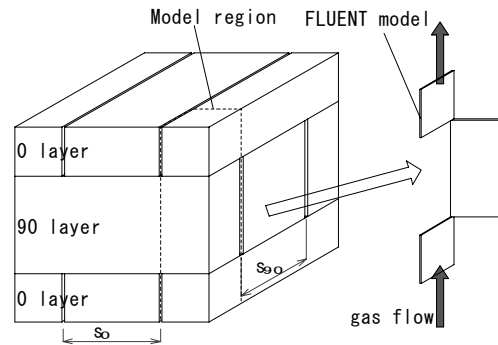


Fig. 6. Modeling of leakage path without crack offset for Fluent

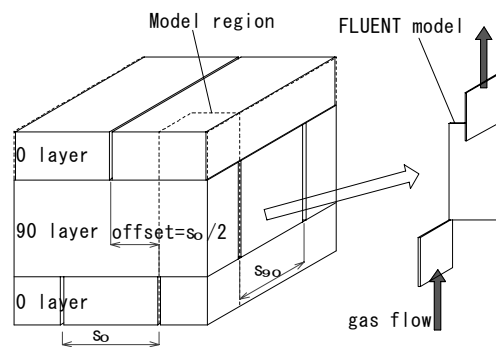


Fig. 7. Modeling of leakage path with crack offset for Fluent

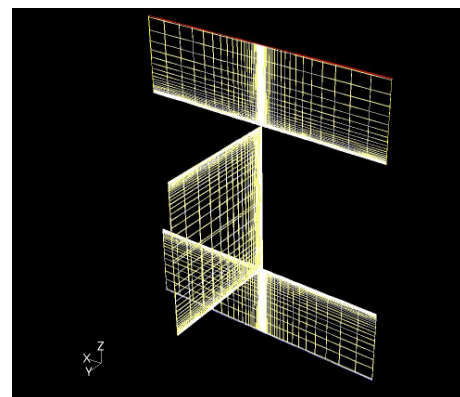


Fig. 8. Grid of CFD model (delamination length = 0.3mm, thermal load, offset=0mm)

delamination was set to be smaller (or larger if the predicted leakage rate was too small). These steps were repeated until the calculated leakage approximately coincided with the experimental results. The delamination size was then used for predicting leakage under biaxial mechanical loadings.

5 Results and Discussions

5.1 Crack Opening Displacements under Thermal Load

The effect of delamination length on crack opening displacements in a 90° layer under thermal load is shown in Fig. 9. In the figure, crack opening

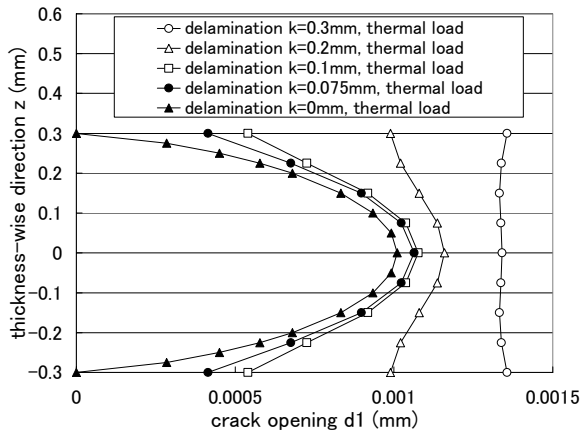


Fig. 9. Crack opening displacements under thermal load (crack in 90 layer)

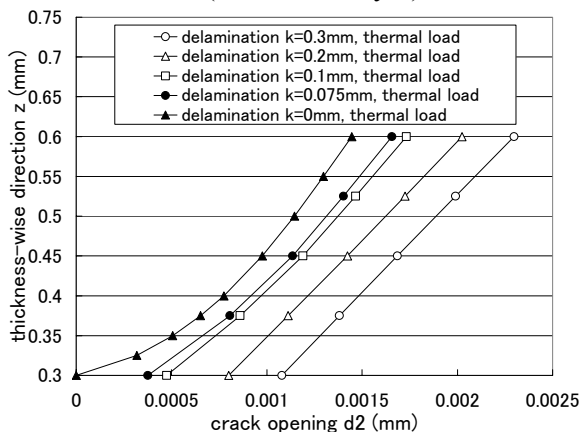


Fig. 10. Crack opening displacements under thermal load (crack in 0 layer)

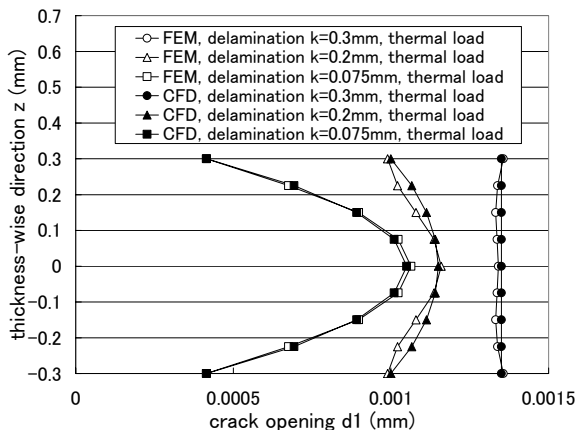


Fig. 11. Comparison of crack opening displacements under thermal load between FEM results and CFD models (crack in 90 layer)

displacements increase as delamination length increases, and the crack opening is nearly flat when the delamination length is 0.3mm. When the delamination length is small, the crack opening displacements are close to those without delamination ($k=0\text{mm}$), which are nearly parabolic.

The effect of delamination length on crack

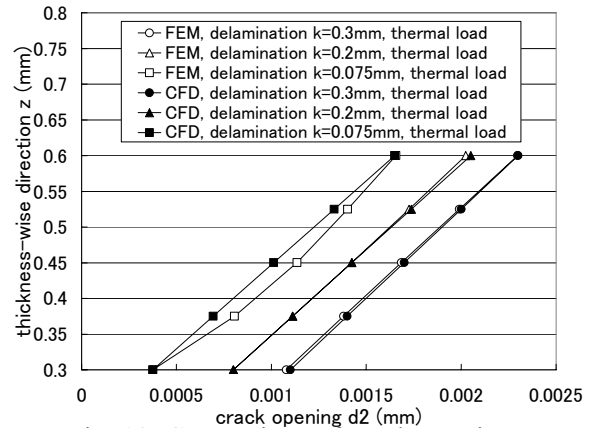


Fig. 12. Comparison of crack opening displacements under thermal load between FEM results and CFD models (crack in 0 layer)

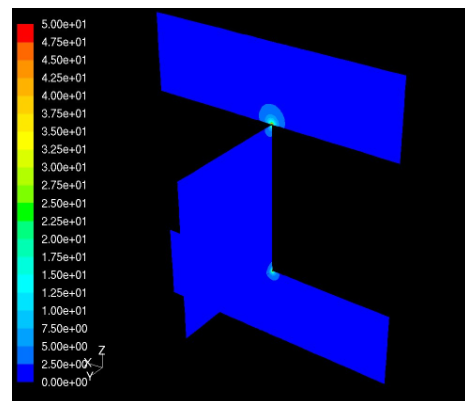


Fig. 13. Velocity magnitude of gas flow through matrix cracks (delamination length = 0.3mm, thermal load, offset=0mm)

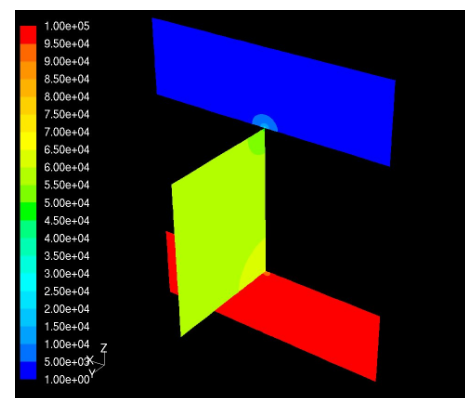


Fig. 14. Pressure magnitude of gas flow through matrix cracks (delamination length = 0.3mm, thermal load, offset=0mm)

opening displacement in a 0° layer under thermal load is shown in Fig. 10. In the figure, the longer the delamination length is, the larger the crack opening. The crack opening displacements are close to those without delamination ($k=0\text{mm}$) when the delamination length is small, similar to the trend in Fig. 9. Crack opening displacements in the CFD

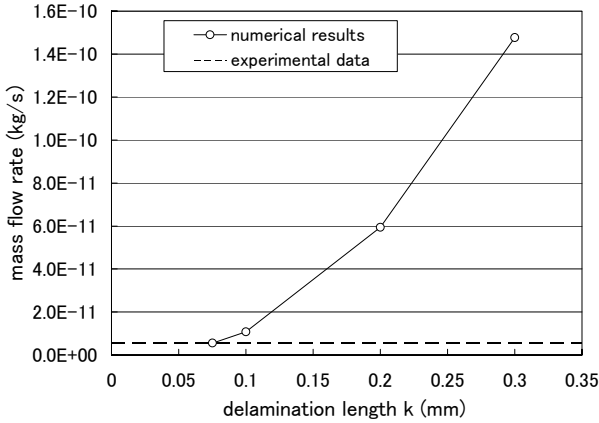


Fig. 15. Relationship between mass flow rate and delamination length (thermal load, offset=0mm)

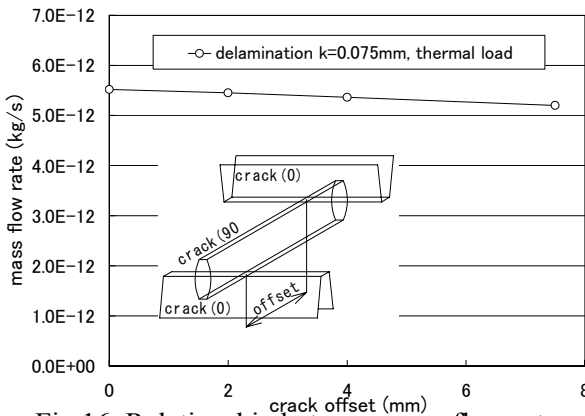


Fig. 16. Relationship between mass flow rate and crack offset (delamination length =0.075mm, thermal load)

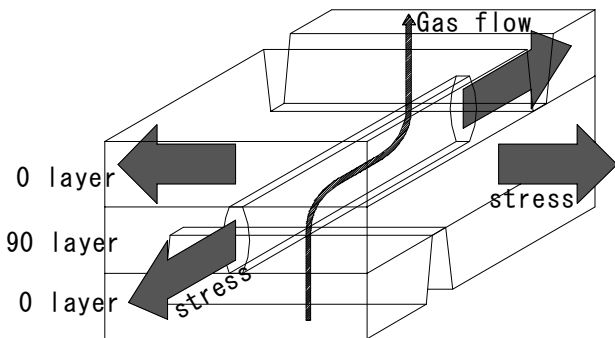


Fig. 17. Leakage through damaged laminate under biaxial stress

model are assumed to be linear or parabolic, as shown in Figs. 11 and 12.

5.2 Leakage under Thermal Load

Figures 13 and 14 show typical contour plots of velocity and pressure through the damage

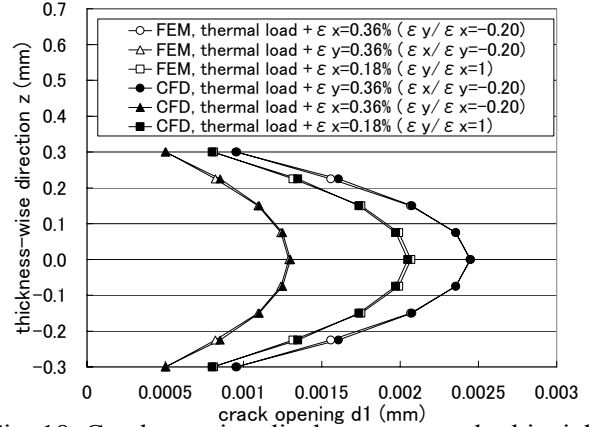


Fig. 18. Crack opening displacements under biaxial load in FEM results and CFD models in 90 layer (delamination length =0.075mm)

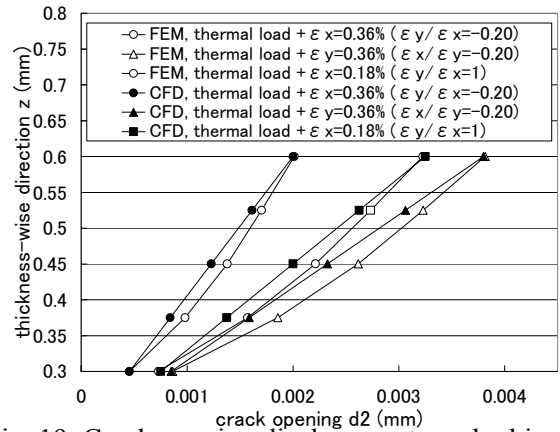


Fig. 19. Crack opening displacements under biaxial load in FEM results and CFD models in 0 layer (delamination length =0.075mm)

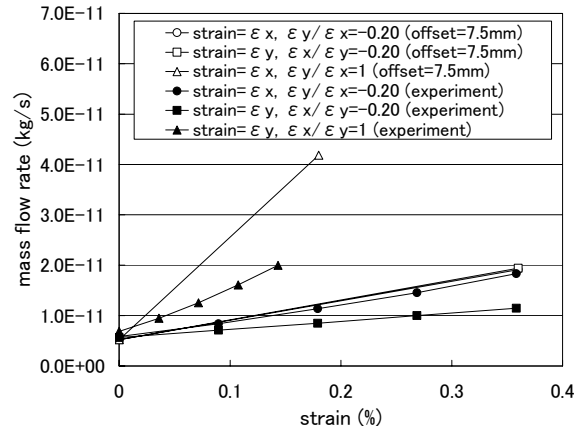


Fig. 20. Comparison of mass flow rate under biaxial load between numerical and experimental results (delamination length =0.075mm)

network without crack offset in the laminate under thermal load. The gas velocity is very high near crack intersections in Fig. 13. A large pressure drop also occurs near the crack intersections, as shown in Fig. 14. The drastic change of gas velocity and pressure near the intersections implies high resistance to gas flow at the intersections of the matrix cracks.

The relationship between mass flow rate under thermal load and delamination length k is shown in Fig. 15. The mass flow rate decreases as the delamination length k decreases. A small delamination length narrows the leakage path and so the resistance is increased. The broken line in Fig. 15 is experimental leakage data under thermal load [9]. From this plot it was deduce that a delamination length $k=0.075\text{mm}$ is appropriate.

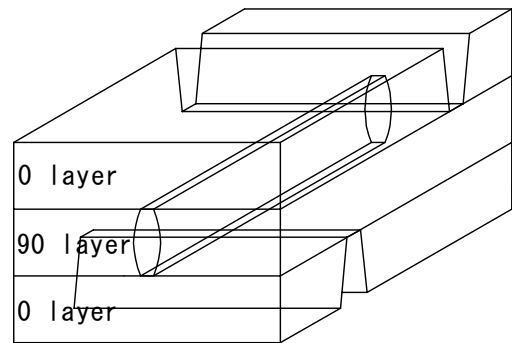
The predictions in Fig. 15 do not include the effect of crack offset. Figure 16 shows the effect of the crack offset with the delamination length $k=0.075\text{mm}$ in the laminate under thermal load. The influence of crack offset on mass flow rate is rather small compared with the effect of delamination length.

5.3 Leakage under Biaxial Loading

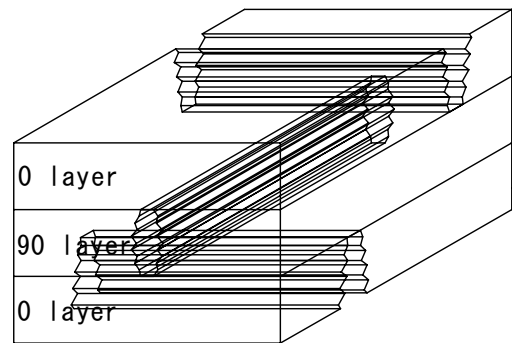
Leakage through damaged laminates under biaxial mechanical loadings (Fig. 17) was calculated in the same way as done previously for the thermal load cases. The delamination length was fixed as 0.075mm based on comparison with the experimental results. The crack spacing in the 0° layer was assumed to be 15mm , which was the average crack spacing in the 0° layer in the experiments [9]. Matrix cracks are assumed to be located at staggered positions (Fig. 7). The crack offset is 7.5mm , which is half of the crack spacing.

Biaxial loading ratios applied to cruciform specimens $F_x:F_y=1:0, 0:1, 1:1$ in the experiments were adopted in this paper, where F_x and F_y are x- and y-directional loading, respectively. Biaxial load ratios $1:0, 0:1$ and $1:1$ correspond to strain ratios $\epsilon_x:\epsilon_y=1:-0.20, -0.20:1$ and $1:1$ in the gauge area, respectively, where ϵ_i ($i=x, y$) is i -directional normal strain. Crack opening displacements under these load ratios with thermal load calculated by FEM and assumed crack opening in CFD models are shown in Figs. 18 and 19. Numerical results of leakage under biaxial mechanical load are compared with experimental results in Fig. 20.

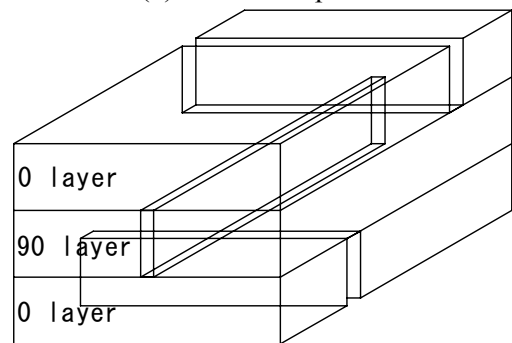
Leakage is a function of strains caused by thermal loading and strains caused by mechanical loading. Relationships between permeability and the



(a) leak path in FEM result (polynomial COD)



(b) actual leak path



(c) leak path with flat crack (constant COD)

Fig. 21. Leak path shapes in damaged laminate

strains caused by the mechanical loading are plotted in Fig. 20, where thermal strains, which were calculated based on the assumed stress free temperature, were fixed.

The crack opening displacements in the model for CFD calculation were assumed as polynomial functions (linear and quadratic functions), and the surfaces of the cracks are smooth like Fig. 21(a). However actual crack surfaces have roughness like Fig. 21(b). In Fig. 20, predicted flow rates are larger than experimental data. The smoothness of the crack surfaces in the CFD model might be the cause of the over-prediction.

The through-crack flow resistance in Fig. 21(b) is expected to be higher than in Fig. 21(a). However,

it is not easy to calculate gas flow through the rough surface cracks like Fig. 21(b).

To approximate the effect of roughness and keep the geometry simple, the crack opening was

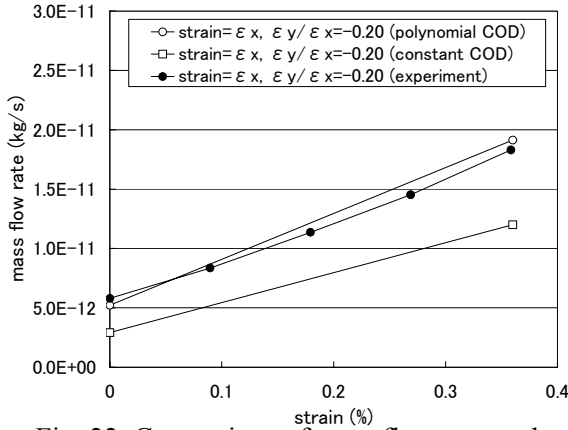


Fig. 22. Comparison of mass flow rate under biaxial load between numerical and experimental results (delamination length = 0.075mm, offset = 7.5mm, $\epsilon_x:\epsilon_y = 1:-0.20$)

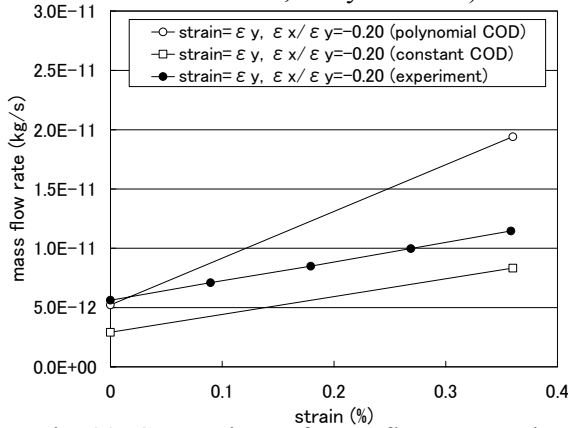


Fig. 23. Comparison of mass flow rate under biaxial load between numerical and experimental results (delamination length = 0.075mm, offset = 7.5mm, $\epsilon_x:\epsilon_y = -0.20:1$)

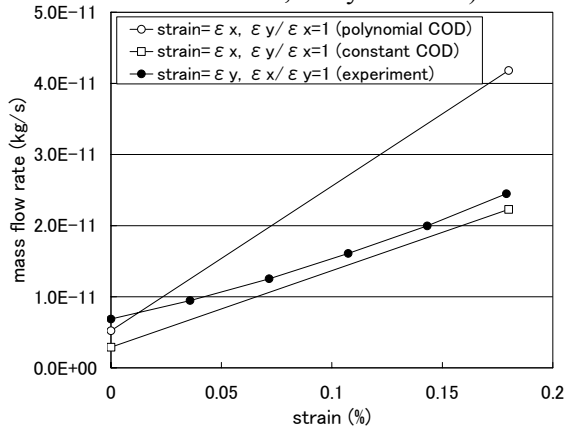


Fig. 24. Comparison of mass flow rate under biaxial load between numerical and experimental results (delamination length = 0.075mm, offset = 7.5mm, $\epsilon_y:\epsilon_x = 1:1$)

assumed to be constant through the thickness. The magnitude of the constant opening was taken to be the same as the opening for the model in Fig. 21(a) at the interface between layers. The models in Fig. 21(a) and (c) are called as polynomial COD (crack opening displacement) model and constant COD model, respectively. The crack opening away from the interlaminar regions in the constant COD model is smaller than that in the polynomial COD model. The smaller crack opening in the constant COD model makes the through-crack resistance higher than the polynomial COD model.

Numerical results of these two CFD models under three strain ratios are compared with experimental data in Figs. 22-24. The experimental data of permeability lies between the results from the polynomial COD model and the constant COD model. It appears that the resistance of the actual leak path is higher than that of the polynomial COD model and lower than that of the constant COD model. The results in Figs. 22-24 indicate that the combination of FEM and CFD can be used to approximately predict leakage under biaxial mechanical loadings based on appropriate delamination length estimated from leakage data under no mechanical load.

6 Conclusions

In this study, numerical models for calculating leakage through damaged laminates were developed by applying FEA for crack opening analysis and by applying CFD for gas flow calculation. Delamination length at crack intersections was estimated based on experimental data obtained for thermal load only. Leakage under biaxial mechanical loadings was predicted using this estimated delamination length. CFD models, in which crack opening displacements were approximated as polynomial (linear and quadratic) functions based on FEA results, were more permeable compared with experimental data under mechanical loadings. The over-prediction of permeability was assumed to be caused by using smooth crack surfaces in the models. Flat crack CFD models with constant COD, which approximated the effect of surface roughness, were less permeable compared with experimental data. However experimental leakage data under biaxial mechanical loadings were bounded by the polynomial COD and the constant COD models. Further investigations are needed to more precisely account for surface roughness.



Acknowledgements

The authors wish to acknowledge Paul Cizmas from Texas A&M University for his invaluable contributions to this research.

References

- [1] Cook S. "The Reusable Launch Vehicle Technology Program and the X-33 Advanced Technology Demonstrator". NASA-TM-111868, 1995.
- [2] Marshall Space Flight Center, NASA. "Final Report of the X-33 Liquid Hydrogen Tank Test Investigation Team", 2000.
- [3] Robinson M.J., Eichinger J.D. and Johnson S.E. "Hydrogen Permeability Requirements and testing for Reusable Launch Vehicle Tanks". *Proceedings of 43rd AIAA /ASME /ASCE /AHS /ASC Structures, Structural Dynamics, and Materials Conference*, AIAA Conference paper 2002-1418, 2002.
- [4] Robinson M.J., Johnson S.E., Eichinger J.D., Hand M.L. and Sorensen E.T. "Trade Study Results for a Second-Generation Reusable Launch Vehicle Composite Hydrogen Tank". *Proceedings of 45th AIAA /ASME /ASCE /AHS /ASC Structures, Structural Dynamics, and Materials Conference*, AIAA Conference paper 2004-1932, 2004.
- [5] Aoki T., Ishikawa T., Kumazawa H. and Morino, Y. "Cryogenic Mechanical Properties of CF/Polymer Composite for Tanks of Reusable Rockets". *Advanced Composite Materials*, Vol. 10, No. 4, pp 349-356, 2001.
- [6] Schoeppner G.A., Kim R. and Donaldson S.L. "Steady State Cracking of PMCS at Cryogenic Temperatures". *Proceedings of 42nd AIAA/ASME/ASCE/AHS/ASC Structures, Structural Dynamics, and Materials Conference*, AIAA Conference paper 2001-1216, 2001.
- [7] Kumazawa H., Hayashi H., Susuki I. and Utsunomiya T. "Damage and permeability evolution in CFRP cross-ply laminates". *Composite Structures*, Vol. 76, No. 1-2, pp 73-81, 2006).
- [8] Kumazawa H., Aoki T. and Susuki I. "Influence of stacking sequence on leakage Characteristics through CFRP composite laminates". *Composites Science and Technology*, Vol. 66, No. 13, pp 2107-2115, 2006.
- [9] Kumazawa H., Aoki T., Susuki I. "Analysis and Experiment of Gas Leakage through Composite Laminates for Propellant Tanks". *AIAA Journal*, Vol. 41, No. 10, pp 2037-2044, 2003.
- [10] Kumazawa H., Aoki T., Susuki I. "Gas Leakage Evaluation of CFRP Cross-Ply Laminates under Biaxial Loadings". *Journal of Composite Materials*, Vol. 40, No. 10, pp 853-871, 2006.
- [11] Humpenoder J. "Gas permeation of fibre reinforced plastics". *Cryogenics*, Vol. 38, pp 143-147, 1998.
- [12] Bechel V.T., Negilski M. and James J. "Limiting the permeability of composites for cryogenic applications". *Composites Science and Technology*, Vol. 66, No. 13, pp 2284-2295, 2006.
- [13] Yokozeki T., Ogasawara T. and Ishikawa T. "Evaluation of gas leakage through composite laminates with multilayer matrix cracks: cracking angle effects". *Composites science and technology*, Vol. 66, No. 15, pp 2815-2824, 2006.
- [14] Roy S. and Benjamin M. "Modeling of permeation and damage in graphite/epoxy laminates for cryogenic fuel storage". *Composites Science and Technology*, Vol. 64, No. 13-14, pp 2051-2065, 2004.
- [15] Roy S., Utturkar A., and Benjamin M. "Modeling of Permeation and Damage in Graphite/Epoxy Laminates at Cryogenic Temperatures". *Proceedings of 45th AIAA /ASME /ASCE /AHS /ASC Structures, Structural Dynamics, and Materials Conference*, AIAA Conference paper 2004-1860, 2004.
- [16] Peddiraju P., Noh J., Whitcomb J. and Lagoudas D.C. "Prediction of Cryogen Leak Rate through Damaged Composite Laminates". *Journal of Composite Materials*, Vol. 41, No. 1, pp 41-71, 2007.
- [17] Noh J. and Whitcomb J. "Effect of various parameters on the effective properties of a cracked ply". *Journal of Composite Materials*, Vol. 35, No. 8, pp 689-712, 2001.
- [18] Nairn J.A. and Hu S. "The Formation and Effect of Outer-Ply Microcracks in Cross-Ply Laminates: a Variational Approach". *Engineering Fracture Mechanics*, Vol. 41, No. 2, pp 203-221, 1992.
- [19] Kobayashi S., Terada K. and Takeda N. "Evaluation of long-term durability in high temperature resistant CFRP laminates under thermal fatigue loading". *Composite Part B*, Vol. 34, No. 8, pp 753-759, 2003.